

실리콘 고무로 개질된 에폭시/클레이 나노복합체의 경화속도론 및 화학유변학

이상목[†]

단국대학교 화학공학과

(2019년 10월 28일 접수, 2019년 12월 7일 수정, 2019년 12월 23일 채택)

Cure Kinetics and Chemorheology of Silicone Rubber Modified Epoxy/Clay Nanocomposites

Sangmook Lee[†]

Division of Chemical Engineering, Dankook University, 126 Jukjeon-dong, Suji-gu, Gyeonggi-do 16890, Korea

(Received October 28, 2019; Revised December 7, 2019; Accepted December 23, 2019)

초록: 실리콘 고무로 개질된 에폭시/클레이 나노복합체의 경화 거동을 미분주사열량계(DSC)와 진동 레오미터를 이용하여 연구하였다. 지환형 에폭시 수지, 아민기를 포함하는 실리콘 고무, 무수 경화제, 나노클레이의 반응을 통해 나노복합체를 제조하였다. 클레이 함량이 4 phr로 증가함에 따라 경화 속도는 증가하였고 반응열은 감소하였으며 젤화 시간은 감소하였다. 등온경화 실험의 결과는 개선된 Kamal 모델에 잘 부합하였다. 이에 개선된 Kamal 모델을 적용하여 본 시스템의 전체적인 경화특성을 모사할 수 있으리라 사료된다.

Abstract: The curing behavior of silicone rubber modified epoxy/clay nanocomposites was studied using a differential scanning calorimeter (DSC) and an oscillatory rheometer. The nanocomposites were prepared from the reaction of cycloaliphatic epoxy resins, silicone rubber containing amine functional group, anhydride hardener and nano-clay. As the clay content increased until 4 phr, the curing reaction rate increased, the reaction heat decreased, and the gelation time decreased. The isothermal cure results were well matched with the modified Kamal's model. Therefore, it is thought that the overall cure characteristics can be simulated by applying a modified Kamal's model.

Keywords: silicone rubber, cycloaliphatic epoxy, cure kinetics, chemorheology, nano-clay.

Introduction

Epoxy resin has excellent mechanical, chemical, and electrical properties, and is a great general-purpose material widely used as electrical and electronic materials and aerospace composite materials. Due to its brittle properties, however, many studies have been carried out to improve it.¹⁻⁴ As part of such efforts, additions of various rubbers to it or its reactions with high molecules of silicone or urethane were attempted.⁵⁻⁷ In particular, there has been a lot of research recently on the copolymerization of siloxane and epoxy.⁸⁻¹⁰ However, the copolymerization of siloxane is complex in the reaction process and requires very demanding management, such as a number of processes, for immediate application and utilization in the field.

The properties of epoxy resin are predetermined by the chemical structure of resin and hardener before curing as well as the network structure after curing. Therefore, the type and structure of the segments that make up the molecular chain, and the cure conditions during processing have a significant influence on the network structure. In order to optimize the physical characteristics of the final product by controlling the reaction in the commercial process, the curing rate and reaction activation energy at different temperatures should be known. Thus, the study of curing kinetics is essential to investigate the relationship between the structure and properties of epoxy resin. The reaction kinetics studies have been mainly reported using spectroscopic instruments such as FTIR, NMR, and Raman¹¹⁻¹³ and the thermal decomposition reaction kinetics has been studied using TGA.¹⁴⁻¹⁶ DSC has been also widely used to study the exothermic curing reaction of thermosetting resin.¹⁷⁻¹⁹

In this study, the modified epoxy resin with flexible siloxane segment was manufactured by reacting the cycloaliphatic

[†]To whom correspondence should be addressed.
s_mlee@naver.com, ORCID[®]0000-0001-8965-3590
©2020 The Polymer Society of Korea. All rights reserved.

epoxy resin with the commercial liquid silicone resin containing amine functional groups. Then, anhydride hardener, imidazole catalyst, and nano-clays were added to it and its curing behavior was investigated using DSC and oscillatory rheometer. In the future, the thermal and mechanical properties and morphology of the cured samples will also be studied.

Experimental

Materials. The epoxy resin used in this study was cycloaliphatic type ES602 of Hajin Chemtec Co. with epoxy equivalence of 164~177 g. The liquid silicone resin was DC3055 of Dow Corning with amine equivalence of 250~270 g. The HJ5500 (methyl hexahydrophthalic anhydride) of Hajin Chemtec Co. with equivalence of 166 g was used as a curing agent. 1-cyanoethylene-2-ethyl-4-methyl imidole (2E4MZ-CN) of Shikoku Kasei, Japan was used as an accelerator. Nano-clay was Cloisite 30B (Southern Clay, USA). All materials in this study were used without further purification and the chemical structures are shown in Figure 1.

Nanocomposite Preparation. Silicone resin and epoxy resin were preheated at 50 °C and mixed at 500 rpm for 10 min. Nano-clay, anhydride hardener, and accelerator were added to it and mixed for another 5 min, followed by an ultrasonic treatment using the ultrasonic horn (1500 W, 20 kHz) for 20 min. The bubbles in the mixture were removed in a vacuum oven for 15 min. The mixing ratio of silicone rubber modified epoxy nanocomposite (hereinafter referred to as SEN) in this study is as shown in Table 1. These prepared mixtures were cured according to the heat applied to the differential scanning cal-

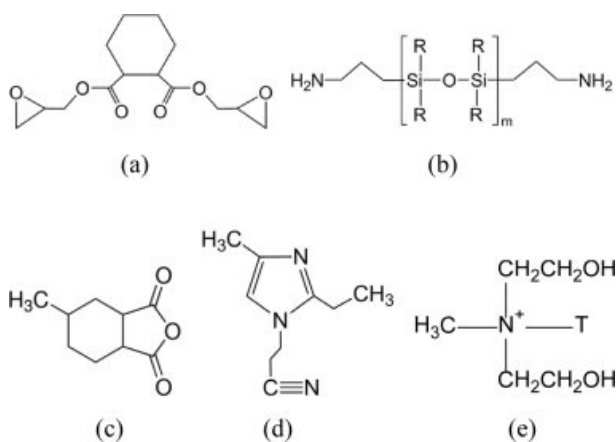


Figure 1. Chemical structures of the materials used in this study: (a) epoxy (ES602); (b) silicone rubber (DC3055); (c) hardener (HJ5500); (d) accelerator (2E4MZ-CN); (e) nano-silicate (cloisite 30B).

orimeter (DSC) and the rheometer measurement. The curing reaction process of above silicone rubber-mixed epoxy resin and anhydride hardener is illustrated in Figure 2.

Instruments. The differential scanning calorimeter (DSC, DSC2910, TA Instrument) was used to measure the thermal behavior by the curing reaction. The prepared uncured specimen was contained about 10±3 mg in a hermetic pan and was dynamically scanned under nitrogen at a rate of 5, 10, 15, 20 °C/min. The isothermal heat curves were also obtained by curing them at 120, 130, 140, 150, and 160 °C.

The rheological measurements were conducted using a stress-controlled rotational rheometer (Physica MCR500, Anton Parr), to examine the viscoelastic properties in terms of the η^* , G' , and G'' . A 25 mm diameter parallel plate was mounted with a gap size of 1 mm. For all specimens, the frequency was 10 rad/s and the temperatures were at 80, 90, 100, and 120 °C.

Table 1. Mixing Ratios (by Weight) of the Nanocomposites

Sample code	Epoxy	Silicone rubber	Hardener	Accelerator	Nano-clay
SEN 0	90	10	88	1	0
SEN 2	90	10	88	1	2
SEN 4	90	10	88	1	4
SEN 8	90	10	88	1	8

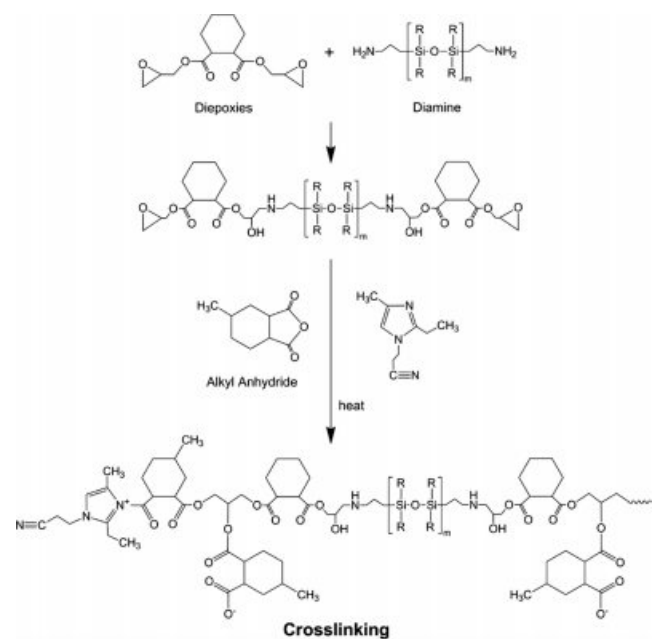


Figure 2. Reaction scheme of silicone rubber modified epoxy with anhydride.

Results and Discussion

Dynamic Curing Kinetics. Figure 3 is the result of thermal analysis of SENs when changing clay content while keeping DSC at a constant heating rate of 15 °C/min. All samples started to release heat at about 75 °C, showed peak near 160 to 170 °C, and stopped heat near 200 to 250 °C. As the clay content increased, the heat peak moved toward lower temperatures and the peak height decreased. This is due to the acceleration effect of the reaction of ammonium and hydroxyl groups on the surface of the clay, resulting in faster reaction as the clay content increased.^{20,21} In addition, at high temperatures, organic ions in the nanocomposite promote homopolymerization²¹ and reduce reaction heat due to reduced crosslinking density.²²

To calculate reaction activation energy from the dynamic DSC data of the SENs, the following expressions were derived by Kissinger.²³

$$-\ln(b/T_p^2) = E_a/RT_p + \text{const} \quad (1)$$

where b is the heating rate (°C/min), T_p is the peak temperature (K) on the DSC curve, and R is the gas constant. This equation was derived under the assumption that the degree of cure at the peak temperature, α_p , is constant regardless of the heating rate, and has been applied to several types of thermosetting resins.^{24,25}

Figure 4 is a Kissinger plot that illustrated $\ln(b/T_p^2)$ as a function of $1000/T_p$ to apply the DSC results with different scanning temperatures to eq. (2). Although there were some errors, the results were generally close to straight lines.

The amount of heat integrated on the peak and the reaction activation energy obtained from the slope of the trend line

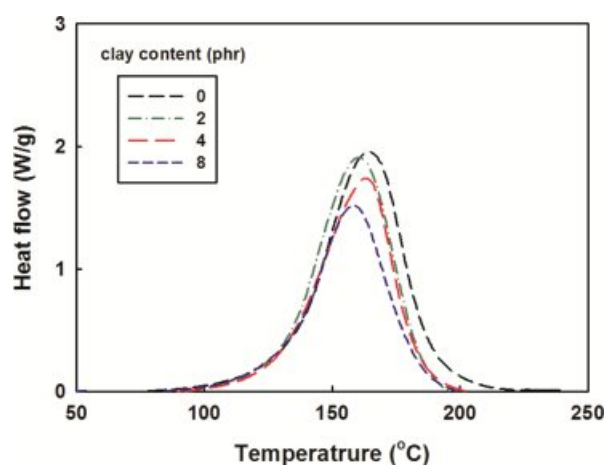


Figure 3. DSC curves of the nanocomposites at different clay contents at a heating rate of 15 °C/min.

were summarized in Table 2. The amount of heat decreased as the clay content increased, while the reaction activation energy was almost the same. It is therefore thought that changes in the content of the clay have little effect on the activation energy.

Degree of cure was obtained by dividing the running integral value of the heat release rate by the total reaction heat, and the results are illustrated in Figure 5. As the temperature increased

Table 2. DSC Results of the Nanocomposites at Different Clay Contents

Sample code	E_a (kJ/mol)	ΔH (J/g)
SEN 0	60.8	304
SEN 2	61.9	293
SEN 4	59.2	272
SEN 8	60.0	245

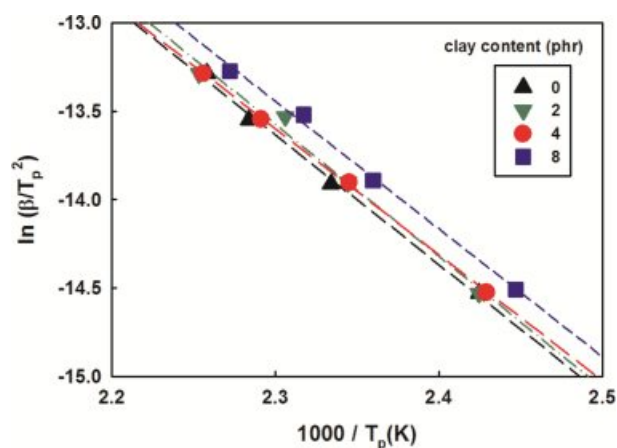


Figure 4. $\ln(b/T_p^2)$ vs $1000/T_p$ of the nanocomposites at different clay contents.

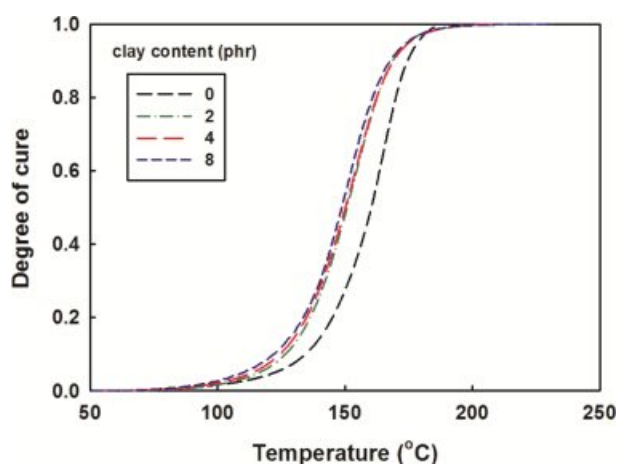


Figure 5. The degree of cure of the nanocomposites at a heating rate of 15 °C/min with varying clay content.

the degree of cure gradually increased in the initial cure stage and then sharply increased to approach 1 at the end. When the clay was added, this phenomenon began at much lower temperatures and the difference according to clay content was not significant.

This temperature shift is attributed to the heat transfer effect due to the addition of clay with high thermal conductivity. When a sample is exposed to heat, the temperature of the entire sample does not reach the set temperature. The more samples you have, the more time it takes for heat to penetrate. Furthermore, polymeric materials take longer due to their low thermal conductivity. However, when a material with a high thermal conductivity is mixed, heat is quickly penetrated and the reaction starts faster.

Isothermal Curing Kinetics. In Figure 6, the DSC thermogram of SEN was illustrated when the clay content was changed while the set temperature of DSC was kept constant at 130 °C. In the initial few minutes the heat flow curves show no tendency, because no matter how much well DSC works, when the cell lid is opened to place the SEN sample in DSC, the isothermal condition is destroyed and it takes time to reach the thermal equilibrium again. Thus, the records in the initial few minutes may appear to be somewhat smaller than the actual heat.

Figure 7 shows the peak time and heat of cure as a function of temperature and clay content. As the temperature increased, the peak time progressed faster and the heat of cure decreased slowly as a whole. It was similar to the dynamic cure reaction analysis. The small picture in Figure 6 shows the changes in heat of cure in more detail as the clay content increased. As the clay content increased, the heat generation decreased dramatically at over 2 phr of clay content, but there was no significant change at over 4 phr of clay content.

The Kamal equation is a phenomenological model that considers the curing reaction of epoxy resin to be an autocatalytic reaction when cured at isothermal.²⁶

$$\frac{d\alpha}{dt} = (k_1 + k_2\alpha^m)(1-\alpha)^n \quad (2)$$

where $k_i = k_{i0}\exp\left(\frac{-\Delta E_{ai}}{RT}\right)$ ($i = 1, 2$)

where k_1 and k_2 are the reaction rate constants for non-autocatalytic and autocatalytic reaction, respectively. m and n are the catalytic constants, k_{10} and k_{20} are the pre-exponential factors, and E_{a1} and E_{a2} are the activation energies.

The curing behavior of the epoxy begins initially with acti-

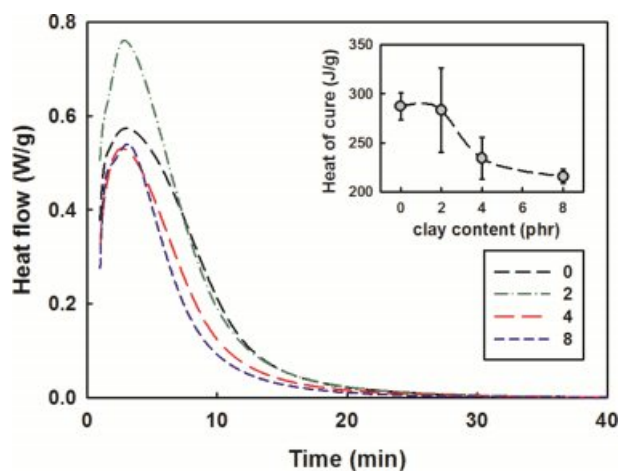


Figure 6. Isothermal DSC curves of the nanocomposites at 130 °C with varying clay content.

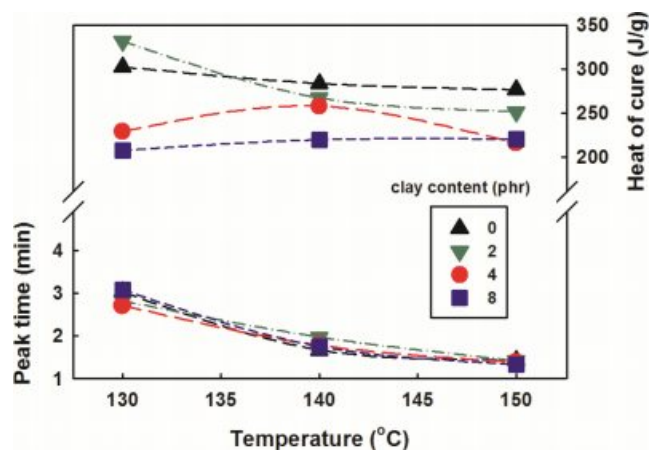


Figure 7. Isothermal peak time and heat of cure vs temperature of the nanocomposites at different clay contents.

vation-controlled reaction, but as the reaction progresses gradually, the mechanism switches to diffusion-controlled. To express this, the modified Kamal's model corrected by introducing the diffusion factor, $f(\alpha)$, is shown in eq. (3).²⁶⁻³⁰

$$\frac{d\alpha}{dt} = (k_1 + k_2\alpha^m)(1-\alpha)^n f(\alpha) \quad (3)$$

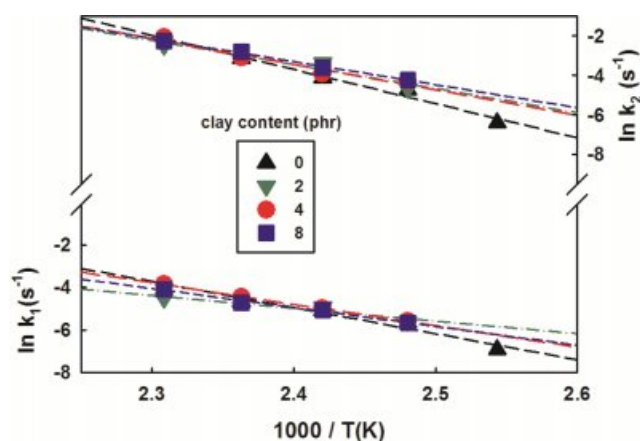
where $f(\alpha) = \frac{2}{1 + \exp(\alpha - \alpha_c)/C} - 1$

where α_c is the maximum degree of cure for a given cure temperature and C is the diffusion parameter.

The values of kinetic variables for the modified Kamal's model were obtained using a multivariable regression method and are listed in Table 3. The higher the temperature, the higher the reaction rate constant k_1 and k_2 were, the more pro-

Table 3. Kinetic Parameters for Modified Kamal's Model of the Nanocomposites

Sample code	T (°C)	k_1 (h ⁻¹)	k_2 (h ⁻¹)	m	n	α_c	C
SEN 0	120	4	6	0.65	0.59	0.88	0.16
	130	13	32	0.91	0.18	0.97	0.99
	140	22	58	0.85	0.26	0.95	0.95
	150	33	157	0.98	0.46	0.94	0.94
SEN 2	130	14	35	0.80	0.18	0.94	1.14
	140	26	126	1.00	0.54	0.92	0.92
	150	25	133	0.60	0.19	0.89	0.89
	160	40	309	0.82	0.39	0.94	0.94
SEN 4	130	13	50	0.81	0.42	0.90	0.90
	140	24	72	0.78	0.32	0.94	0.94
	150	41	162	0.86	0.52	0.87	0.88
	160	77	450	1.14	0.83	0.91	0.91
SEN 8	130	12	53	0.72	0.29	0.90	0.91
	140	22	97	0.69	0.23	0.91	0.91
	150	32	221	0.77	0.51	0.92	0.92
	160	60	376	0.84	0.61	0.94	0.94

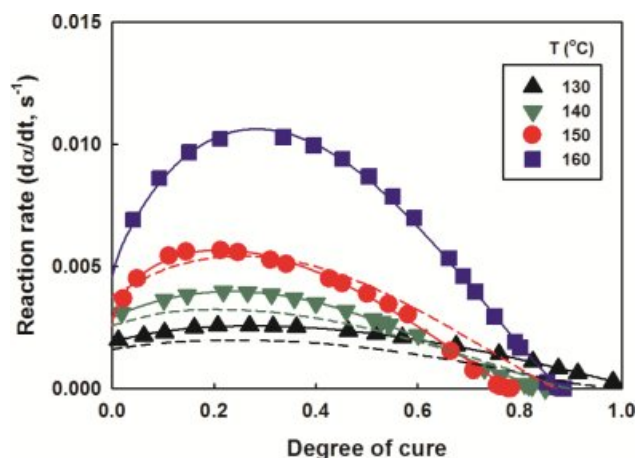
**Figure 8.** Arrhenius plot for the rate constant of the nanocomposites at different clay contents.

nounced the k_2 was. On the other hand, the clay content had little effect on the reaction rate constants. The values of m and n were not constant and had large deviations regardless of the clay content. α_c showed a value between 0.87 and 0.97 without a constant tendency. The values of diffusion parameter C were also almost the same regardless of the clay content.

In order to obtain the reaction activation energies and pre-exponential factors, the natural logarithm to the rate constants was taken and their values were plotted against the reciprocal of the temperature, resulting in near straight lines as shown in Figure 8. The reaction activation energies and pre-exponential factors were obtained from the slopes and the intercepts of the

Table 4. Reaction Activation Energy and Pre-exponential Factor of the Nanocomposites at Different Clay Contents

Sample code	E_{a1} (kJ/mol)	E_{a2} (kJ/mol)	$\ln k_{01}$ (s ⁻¹)	$\ln k_{02}$ (s ⁻¹)
SEN 0	102	144	24.5	37.9
SEN 2	50	101	9.4	25.7
SEN 4	84	107	19.3	27.5
SEN 8	74	97	16.4	24.7

**Figure 9.** Rate of cure vs degree of cure of the nanocomposites (clay 2 phr): experimental results (symbol); modified Kamal's model (line). Dashed lines are the simulated results at clay 0 phr.

straight lines respectively and are summarized in Table 4. As the clay content increased, it was seen that the values of reaction activation energies and pre-exponential factors decreased overall.

The reaction activation energies and pre-exponential factors of the cure kinetic equation obtained from the above could be applied to the modified Kamal model to calculate the cure rate. The rate of cure vs. degree of cure of the nanocomposites with a clay content of 2 phr was illustrated in Figure 9, together with the experimental values. As the degree of cure increased, the rate of cure increased, showed the maximum value at around degree of cure 0.3 and decreased again. The higher the cure temperature, the more significantly the rate of cure increased. The results for other contents were omitted due to similar trends, with only differences in reaction rate values. It was thought that these measured values of the curing rate would be somewhat lower than the actual values. It is because the heat released and spread throughout the sample was recorded by DSC before equilibrium was reached.^{31,32} The experimental data of the curing rate were well matched with their calculations using the modified Kamal equation. There-

fore, it is believed that the modified Kamal model well represents the cure process in this study.

Chemorheology. The rheological properties of the nanocomposites were investigated at different temperatures. The changes in the storage modulus G' and the loss modulus G'' during the curing were measured. As shown in Figure 10, the G' and G'' showed a gradual increase over time, then a sharp increase in a particular time zone. This is due to that the molecular mobility decreases gradually as the curing progresses and decreases rapidly as crosslinking between molecules begins. This trend was noticeable when the temperature was higher, and the time when the G' and G'' began to increase rapidly was also shortened, which is thought to be due to the fast reaction at higher temperatures.

As the curing progresses, it is necessary to define the first time a high-molecular weight polymers appears, called the gel point. It is very important to know the gel time of the material that crosslinks in the actual process because it is almost impossible to process after the gelation time due to the very high viscosity. In general, the gel time is defined as the time to reach the inflection point of the change in viscosity or the intersection of the storage modulus G' and the loss modulus G'' , i.e. $\tan \delta = 1$.³³ It also means the transition from a viscous fluid to a viscous solid due to sufficient entanglement in the polymer chain, and the case of the nanocomposite with a clay content of 2 phr at 100 °C is shown in Figure 10. The small picture shows a change in gel time as a function of temperature, which resulted in a decrease according to Arrhenius formula as the temperature increased. The time of gelation according to clay content and temperature was given in Table 5. It could be seen

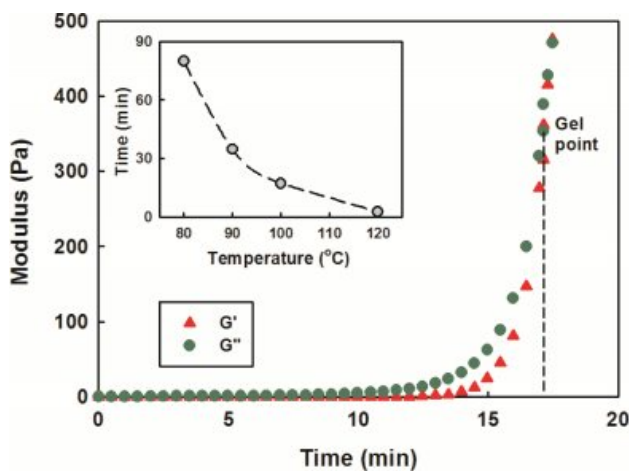


Figure 10. G' and G'' vs time of the nanocomposites (clay 2 phr) isothermally cured at 100 °C.

that the gel time decreased as the cure temperature increased at each content. On the other hand, the gel time decreased as the clay content increased, but increased again when the clay content was 8 phr. It is thought to be due to the catalytic effect of clay as explained in Figure 3 and the role of clay as a heat sinker. In other word, the catalytic effect was dominant in low clay content, but in high clay content, the heat loss was greater, resulting in longer gelation time.

The relationship between gelation time and temperature can be expressed in the form of Arrhenius Law.³⁴

$$k' = k'_0 \exp(-E_a/RT) \quad \text{where } k' \equiv 1/t_{\text{gel}} \quad (4)$$

where k' is the rate constant obtained using gelation time, k'_0 is the pre-exponential factor, E_a is the activation energy, and R is the gas constant. The natural logarithm on both sides of the eq. (4) is as follows.

$$\ln t_{\text{gel}} = -\ln k'_0 + E_a/RT \quad (5)$$

Therefore, the change in the gel time based on the intersections of modulus under isothermal conditions was illustrated as a function of the reciprocal of the temperature in

Table 5. Gel Time (min) and Activation Energy of the Nanocomposites at Different Clay Contents

Sample code	T (°C)				E_a (kJ/mol)
	80	90	100	120	
SEN 0	92	38	17	4	93.0
SEN 2	80	35	17	3	97.7
SEN 4	77	33	16	2	100.4
SEN 8	91	41	22	3	96.1

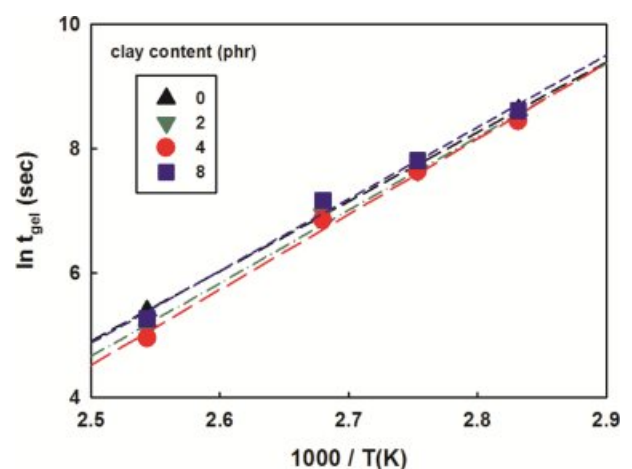


Figure 11. $\ln t_{\text{gel}}$ vs $1000/T$ of the nanocomposites at different clay contents.

Figure 11. As the clay content increased, the intercept of plot decreased, which means shorter gelation time. The activation energies obtained from the slopes were added to Table 5. An increase in activation energy could be seen as clay content increased. The activation energy values obtained here showed some deviation from those obtained using Kissinger equation in the dynamic curing study. This is thought to be due to the amount of samples and the heating mode used in the cure kinetics experiment being different from those used in the chemorheology experiment, resulting in a different heat transfer effect. The amount of samples used in the dynamic cure kinetics is several mg, whereas that in the chemorheology is several g. Therefore, the difference of time lag is inevitable to reach the set temperature. There are also different heating mechanism and temperature sensing mechanism between the two methods.

Conclusions

The curing reaction was made by adding anhydride hardener, nano-clay, and accelerator to the cycloaliphatic epoxy resin modified with the liquid silicon rubber. Using DSC dynamic analysis, the reactivity of the mixture was investigated. As the clay content increased, the curing rate increased, the reaction heat decreased, and the activation energy changed little. Similar results were found in DSC isothermal analysis and the experimental values of isothermal curing reactions were well matched with the calculation of modified Kamal's model. Reactivity was also tested under constant shear rate in a rheometer and the gelation time was shortened as the clay content increased. Therefore, by adding a small amount of nano-clay to the cycloaliphatic epoxy resin modified with silicone rubber, it is believed that the outdoor purpose epoxy nanocomposites with enhanced processibility as well as good flexibility and weather resistance can be obtained.

Acknowledgements: The present research was supported by the research fund of Dankook University in 2019 (No: R201900746). Special thanks are due to Dr. Young Gi Hong for his help with the experiments.

References

1. R. Bagheri, B. T. Marouf, and R. A. Pearson, *Polym. Rev.*, **49**, 201 (2009).
2. L.-X. Gong, L. Zhao, L.-C. Tang, H.-Y. Liu, and Y.-W. Mai, *Compos. Sci. Technol.*, **121**, 104 (2015).
3. H. Zhou and S. Xu, *Mater. Lett.*, **121**, 238 (2014).
4. S. A. Xu, G. T. Wang, and Y. W. Mai, *J. Mater. Sci.*, **48**, 3546 (2013).
5. S. K. Rath, J. G. Chavan, S. Sasane, Jagannath, M. Patri, A. B. Samui, and B. C. Chakraborty, *Appl. Surf. Sci.*, **256**, 2440 (2010).
6. A. A. Prabu and M. Alagar, *Prog. Org. Coat.*, **49**, 236 (2004).
7. T. H. Hsieh, A. J. Kinloch, K. Masania, J. S. Lee, A. C. Taylor, and S. Sprenger, *J. Mater. Sci.*, **45**, 1193 (2010).
8. J. J. Chrusciel and E. Lesniak, *Prog. Polym. Sci.*, **41**, 67 (2015).
9. R. Li, H. Zhang, C. Zhou, B. Zhang, Y. Chen, H. Zou, and M. Liang, *Appl. Polym. Sci.*, **134**, 45272 (2017).
10. B. Li, C. He, W. Lu, J. Wang, Y. Zeng, and B. Gao, *Prog. Org. Coat.*, **126**, 178 (2019).
11. Z. Niu, G. Liu, H. Yin, C. Zhou, D. Wu, B. Yousaf, and C. Wang, *Energ. Convers. Manage.*, **124**, 180 (2016).
12. G. Zheng, L. Polavarapu, L. M. Liz-Marzan, I. Pastoriza-Santos, and J. Perez-Juste, *Chem. Comm.*, **51**, 4572 (2015).
13. M. Cha, K. Shin, H. Lee, I. L. Moudrakovski, J. A. Ripmeester, and Y. Seo, *Environ. Sci. Technol.*, **49**, 1964 (2015).
14. Q.-V. Bach and W.-H. Chen, *Bioresource Technol.*, **246**, 88 (2017).
15. K. Azizi, M. K. Moraveji, and H. A. Najafabadi, *Bioresource Technol.*, **243**, 481 (2017).
16. Y. Lin, Y. Liao, Z. Yu, S. Fang, Y. Lin, Y. Fan, X. Peng, and X. Ma, *Energ. Convers. Manage.*, **118**, 345 (2016).
17. J. Hu, J. Shan, J. Zhao, and Z. Tong, *Thermochim. Acta*, **632**, 56 (2016).
18. J. Xu, Y. Jiang, T. Zhang, Y. Dai, D. Yang, F. Qiu, Z. Yu, and P. Yang, *Prog. Org. Coat.*, **122**, 10 (2018).
19. J. D. Thanki and P. H. Parsania, *J. Therm. Anal. Calorim.*, **130**, 2145 (2017).
20. J. Park and S. C. Jana, *Polymer*, **45**, 7673 (2004).
21. S. K. Sahoo, S. Mohanty, and S. K. Nayak, *Prog. Org. Coat.*, **88**, 263 (2015).
22. P. I. Xidas and K. S. Triantafyllidis, *Eur. Polym. J.*, **46**, 404 (2010).
23. H. E. Kissinger, *Anal. Chem.*, **29**, 1702 (1957).
24. X. Sheng, M. Akinc, and M. R. Kessler, *J. Therm. Anal. Calorim.*, **93**, 77 (2008).
25. G. Gheno, R. Ganzerla, M. Bortoluzzi, and R. Paganica, *Prog. Org. Coat.*, **78**, 239 (2015).
26. M. R. Kamal and M. E. Ryan, *Polym. Eng. Sci.*, **20**, 859 (1980).
27. N. Rabearison, Ch. Jochum, and J. C. Grandidier, *J. Mater. Sci.*, **46**, 787 (2011).
28. F. X. Perrin, T. M. H. Nguyen, and J. L. Vernet, *Eur. Polym. J.*, **43**, 5107 (2007).
29. C. D. Han and K. W. Lem, *Polym. Eng. Sci.*, **24**, 473 (1984).
30. K. C. Cole, J. J. Hechler, and D. Noel, *Macromolecules*, **24**, 3098 (1991).
31. S. Montserrat, G. Andreu, P. Cortes, Y. Calventus, P. Colomer, J. M. Hutchinson, and J. Malek, *J. Appl. Polym. Sci.*, **61**, 1663 (1996).
32. R. A. Fava, *Polymer*, **9**, 137 (1968).
33. Cure behavior by dynamic mechanical analysis ASTM D4473.
34. H. Teil, S. A. Page, V. Michaud, and J.-A. E. Manson, *J. Appl. Polym. Sci.*, **93**, 1774 (2004).